Electron transport through single organic molecules and self-assembled monolayers

Huisman, Everardus Hendrik

Chapter 5

Interpretation of transition voltage spectroscopy

The promise of 'transition voltage spectroscopy' (TVS) is that molecular level positions can be determined in molecular devices without applying extreme voltages. Here, we consider the physics behind TVS in more detail. Remarkably, we find that the Simmons model employed thus far is inconsistent with experimental data. However, a coherent molecular transport model does justify TVS as a spectroscopic tool. Moreover, TVS may become a critical test to distinguish molecular junctions from vacuum tunnel junctions.[1]

5.1 Transition voltage spectroscopy

Over the last decade, several methods have been developed to fundamentally study charge transport in metal-molecule-metal junctions [42, 50, 121, 122]. Nevertheless, much of the physics behind molecular transport is still under debate. In fact, simple questions such as "Where does the voltage drop in a molecular junction?" and "Where are the molecular levels with respect to the electrodes' Fermi levels?" have not found general solutions yet. The latter question, for example, is hard to answer experimentally due to the limited voltage a two-terminal molecular junction can withstand. In a molecular device, the Fermi level (E_F) of the metal electrodes is typically a few eV away from the closest molecular level (see figure 5.1a,e). Therefore, a bias voltage up to several volts is required before electrons from the metal can resonantly flow through a molecular level ('resonant tunneling'). Generally, such voltages result in huge electric fields, $> 10^9$ V/m, causing breakdown before the molecular level is actually accessed. Recently, Beebe *et al.* found a creative way out of this dilemma [123, 124]. They state that the position

[1] This work has been previously published as E.H. Huisman, C.M. Guédon, B.J. van Wees and S.J. van der Molen Nano Lett. **9** 3909 (2009).

of the nearest molecular level in a two-terminal device can be derived from I-V (current-voltage) measurements, even if the bias voltage is moderate and resonance is not yet reached. All that is needed is to replot of the I-V data in a form that is based on the physics of field emission. Due to its simplicity and elegance, this method, coined 'transition voltage spectroscopy' (TVS), is becoming a very popular tool in molecular electronics [125, 126, 127, 128, 129]. However, a basic justification is still lacking. This chapter is therefore devoted to the physical interpretation of TVS. Beebe *et al.* employ the Simmons model for tunneling to interpret their data and justify TVS [130]. Surprisingly, we find that the experimental results they present are not at all in agreement with this model. We show that a coherent molecular transport model, however, does justify their approach. This opens the road for TVS to become an important tool in molecular transport.

To introduce TVS, we initially follow the approach by Beebe *et al.*. They make the analogy between molecular charge transport and electron tunneling through a rectangular barrier, as described by Simmons (see figure 5.1a-d) [130, 131]. Within this framework, the height of the tunnel barrier, ϕ, equals the energy offset between E_F and the nearest molecular orbital. For thiol-terminated molecules, the nearest level is commonly the highest occupied molecular orbital (HOMO, with energy E_{HOMO}), so that $\phi = E_F - E_{HOMO}$ (hole transport) [32, 123, 124]. The barrier width, d, is set equal to the length of the molecule. Simmons showed that for bias voltages $V < \phi/e$ with e the electron charge, the effective tunnel barrier is lowered to $\phi - eV/2$ (see figure 5.1c). However, for high biases, $V > \phi/e$, the barrier shape becomes triangular and part of the barrier becomes classically available. This case is generally referred to as Fowler-Nordheim tunneling (FN) or field emission [132]. Figure 5.1d illustrates the transition between both regimes, at $V = \phi/e$. In the FN-regime, I is related to V by $I \propto V^2 exp(c/V)$, where $c < 0$ depends on the thickness and height of the barrier. Hence, plots of $ln(I/V^2)$ versus $1/V$ (FN-plots) yield a straight line with a negative slope, provided $V > \phi/e$. Beebe *et al.* took the original approach to extend this way of plotting I-V data to low V. Interestingly, such FN-plots yield a well-defined minimum at a voltage V_m. Intuitively, the existence of this minimum is easily understood. Since $I \propto V$ at low biases ($V \ll \phi/e$), an FN-plot of $ln(I/V^2) \propto ln(1/V)$ vs $1/V$ must yield a positive slope at low V (high $1/V$). At high biases, the slope is negative and thus a minimum appears in between. In fact, any $I(V)$-curve that evolves from linear to more than quadratic will have a minimum in a FN plot. Referring to the Simmons model, Beebe *et al.* suggest that: (i) V_m scales linearly with $\phi = E_F - E_{HOMO}$ (or $E_{LUMO} - E_F$, where LUMO denotes lowest unoccupied molecular level); (ii) V_m is independent of molecular length d for constant ϕ; (iii) V_m equals the voltage at which there is a transition to the FN regime (hence 'transition voltage', see figure 5.1d) [123, 124]. Their striking experimental results substantiate

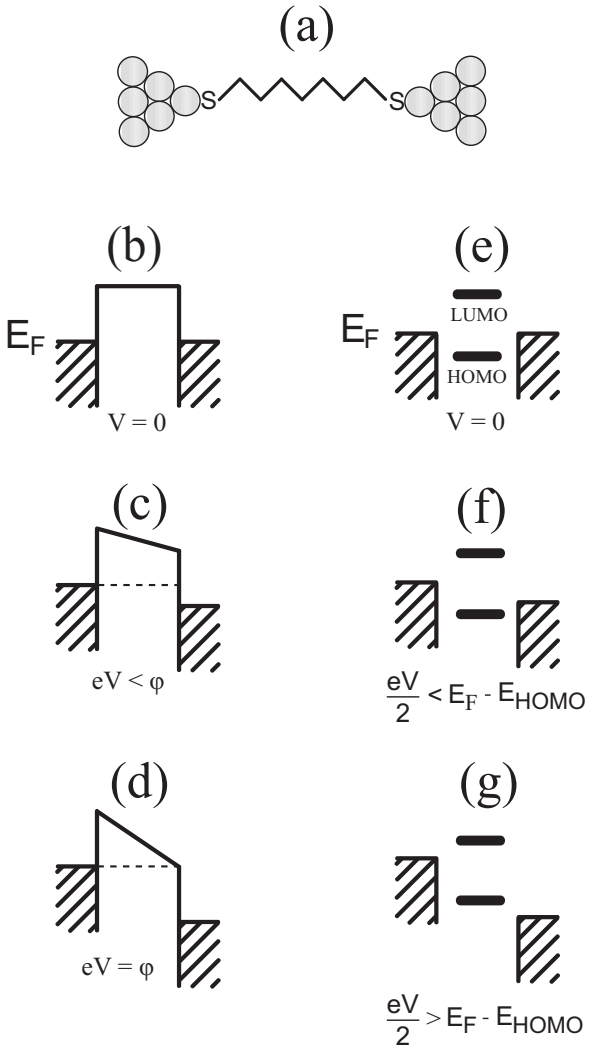

Figure 5.1: **(a)**: molecular junction (thiol bonds). **(b)-(d)**: Simmons model. Here, a molecule is depicted as a tunnel barrier of height ϕ and length d (**(b)**, for clarity we picture electron tunneling only). Upon applying a bias voltage, the barrier is tilted (**(c)**). When $eV \geq \phi$, the barrier becomes triangular and electrons tunnel by field emission (**(d)**). **(e)-(g)**: resonant molecular model. Here, the molecular levels are broadened by the interaction with the electrodes (**(e)**). At elevated biases, the left and right chemical potentials open a window for transport of size eV (**(f)**). The current increases dramatically when a level is within the bias window (**(g)**, resonant tunneling).

these propositions. Measurements on self-assembled monolayers (SAMs) of a variety of conjugated molecules show that $V_m \propto E_F - E_{HOMO}$, where the latter difference is determined by photoelectron spectroscopy. Furthermore, they find V_m to be independent of molecular length, d, for alkanethiols. This is consistent with the fact that the HOMO-LUMO gap of these molecules is virtually length independent [124]. All these important observations make a strong case for TVS to become a general technique in molecular electronics. We therefore start our study by investigating the Simmons model, put forward by Beebe *et al.*, in detail. Surprisingly, we find that it is in strong disagreement with the experimental data in Refs. [123, 124]. To demonstrate this, we first make use of a simple, but rather accurate analytical model for tunneling. This has the advantage that we can obtain a simple analytical expression for V_m. Subsequently, we confirm this result by using the full Simmons model numerically.

5.2 Simmons revisited

To describe electron tunneling in an elegant manner, we use a reformulation of Stratton's formula for direct tunneling [39, 133]. This gives $I(V)$-curves of the form:

$$I \propto sinh(\frac{eV\tau}{\hbar}) \tag{5.1}$$

Here, $\tau = d\sqrt{m/2\phi}$ is the tunnel traversal time and m is the electron mass. Previously, a comparison between Simmons and Stratton was made by Hartman [134]. Due to the simple form of equation 5.1, it is straightforward to determine an analytical expression for V_m (see appendix B):

$$\frac{1}{V_m} = \frac{e\tau}{2\hbar} coth(\frac{eV_m\tau}{\hbar}) \tag{5.2}$$

It is very instructive to discuss an approximate solution to equation 5.2. For this, let us assume that $eV_m >> \hbar/\tau$, such that $coth(eV_m\tau/\hbar) = 1$. Then:

$$V_m \approx \frac{2\hbar}{e\tau} = \frac{2\hbar}{e\sqrt{m}} \frac{\sqrt{2\phi}}{d} \tag{5.3}$$

Before we discuss equation 5.3, we check its validity by substituting it back into equation 5.2. This yields $coth(e\tau V_m/\hbar) = coth(2) = 1.037$, so that equation 5.3 is accurate within a few per cent.

Equation 5.3 is remarkably different from the results Beebe *et al.* obtained: (i) V_m is not proportional to the barrier height, but to its square root; (ii) V_m is not independent of the molecular length d, but inversely proportional to it; (iii) there is no general correspondence between V_m and the transition voltage at which a tunnel barrier becomes triangular (depicted

in figure 5.1d). The latter voltage equals ϕ/e, *independent of* d, whereas equation 5.3 yields $V_m \propto 1/d$.

Clearly, the Stratton approach is only an approximation. Nevertheless, equation 5.3 turns out to have more general validity. To show this, we turn to the actual Simmons model. In our calculations, we include the integrals that are neglected in Ref. [130] itself. This prevents unphysical results for short and low barriers, a common problem in tunneling analysis (see appendix B).

We proceed our discussion in the light of the most elaborate and convincing result Beebe *et al.* present. They perform TVS on a series of alkanethiol molecules with lengths ranging from 9 to 24 Åand find $V_m = 1.2V$, almost independent of molecular length. Since alkanes have become a benchmark system in experimental transport studies, they form a perfect test bed for our present study as well [32, 42, 56, 58, 59, 87, 89, 91, 124, 131]. There is general agreement that $\phi = E_F - E_{HOMO}$ hardly changes with alkane length. However, for its precise value different numbers can be found in literature, even in the well-studied case of Au-S coupling [42, 131, 32]. In the following, we use $\phi = 4eV$ [131]. For generality, however, all calculations presented below have also been performed for values, $\phi = 2.14eV$, taken from Ref. [32], and $\phi = 3eV$ (see appendix B).

The inset of figure 5.2a shows an $I(V)$-curve for a rectangular barrier with $\phi = 4$ eV and $d = 10$ Å, computed by the Simmons expression for the intermediate regime (eV$< \phi$). The corresponding FN-plot (main panel in figure 5.2a), exhibits a clear minimum around $V_m = 1.5V < \phi/e$. Thus, we have the tools at hand to test equation 5.3 for the Simmons model. In figure 5.2b, we show V_m vs. $\sqrt{\phi}$ for a virtual series of ϕ-values, assuming constant length d=10 Å. As anticipated above, we see that $V_m \propto \sqrt{\phi}$.

Next, we plot V_m for a series of lengths d, with $\phi = 4eV$ (see figure 5.2c, blue line). Indeed, we find that $V_m \propto 1/d$. In fact, the Simmons result deviates very little from the line obtained using the Stratton approach (black in fig 5.2c). We conclude that equation 5.3 approximately holds for the Simmons model as well. Most importantly, however, these calculations confirm that there is a large discrepancy between data and model, as presented for TVS thus far [123, 124]. Hence, a new interpretation of TVS is due. Two different approaches can be considered for this. The first is to extend the Simmons model to include the image potential. The influence of the latter is that the effective barrier height ϕ decreases considerably [130, 131]. Since this effect is larger for shorter molecules, this may locally cancel the length dependence in equation 5.3. Alternatively, we will consider a coherent transport picture based on molecular levels, Lorentz-broadened by coupling to the leads. In that case, the voltage is assumed to drop fully at both metal-molecule contacts. This is in strong contrast with any type of Simmons model, where the voltage drops evenly over the junction (see fig 5.1).

To include the image force, we follow Simmons without neglecting terms

[130]. For the local dielectric constant, we take $\epsilon_r = 2.1$ [135, 150]. Figure 5.2c shows V_m as a function of $1/d$. For large d (small $1/d$), this result deviates little from the bare Simmons result. For smaller d, however, it differs considerably. In fact, a maximum in $V_m(d)$ is seen, which indeed results from a decrease of the barrier height as the electrodes come closer to each other. Nevertheless, for the length scales that Beebe *et al.* investigated (9 to 24 Å), V_m is still strongly dependent on d. Hence, we cannot explain the experimental data by including the image potential in a Simmons model.

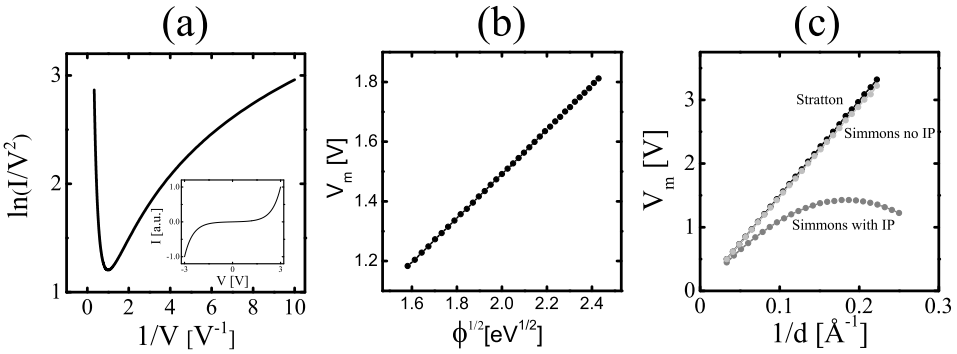

Figure 5.2: **(a)**: Fowler-Nordheim plot for a barrier with $\phi = 4eV$ and $d = 10$ Å, as predicted by the Simmons model. V_m is determined from the minimum of the graph. Inset: corresponding $I(V)$-curve on a linear scale. **(b)**: V_m versus $\sqrt{\phi}$ for the Simmons model ($d = 10$ Å). The linear relation is consistent with equation 5.3. **(c)**: V_m versus $1/d$ for $\phi = 4eV$, using various tunnel models. Black: Stratton model (equation 5.3). grey: full Simmons model without image potential. light grey: full Simmons model including image potential ($\epsilon_r = 2.1$). Clearly, V_m depends strongly on d in all cases.

5.3 An alternative picture

Let us consider a more common picture of a molecular junction, as sketched in figure 5.1e-g [136, 137, 138, 139, 140]. The molecular levels are located below (occupied) and above (empty) the Fermi energy of the metal contacts. Within the coherent Landauer approach, transport through such a junction is described by a transmission function T(E) that depends explicitly on energy. This function is peaked around the molecular levels. In fact, it has been extensively shown that a Lorentzian provides a good description for the transmission around a single molecular level [136, 137, 140]. Resonant tunneling can be achieved by applying the proper gate voltage in three-terminal junctions. In two-terminal devices, however, resonant tunneling is only pos-

sible by opening a voltage window eV high enough for the molecular level to fall in between the left and right chemical potentials (see figure 5.1g). As discussed above, a device typically breaks down before this point is reached. Here, we will assume that one molecular level (HOMO) dominates transport, as is often the case in molecular junctions [32, 123, 124]. Thus our model captures the most relevant physics needed for an analysis of TVS. For $T(E)$, this yields:

$$T(E) = \frac{\eta(1-\eta)\Gamma^2}{\Gamma^2/4 + (E-\varepsilon)^2} \tag{5.4}$$

where $\varepsilon = E_{HOMO}$ (we set $E_F = 0$). Furthermore, $\Gamma = \Gamma_1 + \Gamma_2$ denotes the total energy broadening due to the coupling between metal and electrodes. Specifically, $\Gamma_1 = \eta\Gamma$ and Γ_2=(1-η)Γ describe the overlap between the molecule and the left and right electrode, respectively. The parameter η denotes the asymmetry of the coupling. Symmetric coupling corresponds to $\eta = 0.5$. In that case, an applied voltage drops symmetrically at the left and right contacts (compare figures 5.1d and 5.1g). The $I(V)$-relationship can be calculated from the Landauer formula:

$$I = \frac{2e}{h}\int_{-\infty}^{\infty} T(E)[f_1(E) - f_2(E)]dE \tag{5.5}$$

Here, $f_{1,2}(E) = (exp((E-\mu_{1,2})/kT) + 1)^{-1}$ is the Fermi function for a temperature T, at the left ($\mu_1 = eV/2$) and right ($\mu_2 = -eV/2$) electrode, respectively.

There is overwhelming experimental evidence that the zero-bias conductance of alkanes, as well as of many conjugated molecules, decreases exponentially with molecular length d. In general, one finds $dI/dV(V = 0) \propto exp(-\beta d)$ where the decay constant β depends on the molecular series considered; β is highest for saturated molecules [42, 121, 141]. Interestingly, this result implies that also $T(E = E_F) \propto exp(-\beta d)$ (see equation 5.5). Indeed, several theory groups have confirmed such a relationship, using tight binding models in combination with (non-equilibrium) Green's function methods [138, 139, 140]. In our model, two free parameters exist, Γ and ε. In principle, both can depend on d. However, for longer alkanes, ε is known to be basically independent of d [131, 142]. Therefore, the length dependence must be in Γ. This has the immediate consequence that $\Gamma(d) \approx \frac{(E_F-\varepsilon)}{\sqrt{\eta(1-\eta)}} exp(-\beta d/2)$, using the fact that $E_F - \varepsilon >> \Gamma$ for longer alkanes. This relationship is consistent with extensive calculations by Samanta *et al.* for a series of oligophenyl molecules [140]. We note furthermore that Malen *et al.* applied a similar expression for Γ(d) to successfully describe their experimental data [141]. Upon substituting Γ(d) in equation 5.4, a length dependent transmission function is obtained:

$$T(E,d) = \frac{1}{\frac{1}{4\eta(1-\eta)} + (\frac{E-\varepsilon}{E_F-\varepsilon})^2 exp(\beta d)} \tag{5.6}$$

Combining eqs. 5.5 and 5.6, we can calculate $I(V)$-curves for a series of molecular lengths and determine V_m. To compare to experimental data on alkanethiols, we take T= 300 K, $\varepsilon = -4eV$ and $\beta = 0.74\text{Å}^{-1}$ from extended literature [42]. Figure 5.3a shows T(E) for several alkane lengths, whereas the inset of figure 5.3b displays the corresponding FN plots. The length dependence of V_m is given in the main panel of figure 5.3b. Remarkably, V_m is independent of molecular length for $d > 8$Å. This is fully in agreement with the data of Beebe *et al.*, who find V_m to be independent of length for alkanes longer than 9Å[124]. We note in addition that we find $V_m \propto \phi$ for a range of realistic values of ϕ (see appendix B). We come to the important conclusion that TVS does indeed give us direct information on the molecular levels, as Beebe *et al.* have suggested. However, the interpretation of TVS only works within the framework of a coherent molecular transport model. Simmons-like pictures are inconsistent with experiments on molecular junctions.

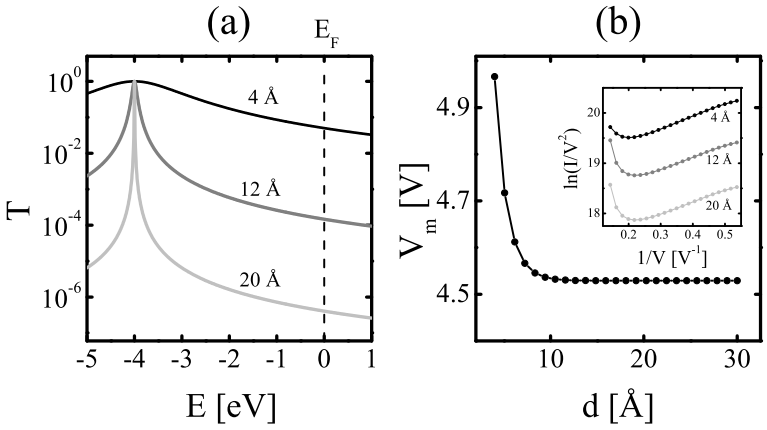

Figure 5.3: Resonant molecular transport model applied to alkane junctions (see figure 5.1a). **(a)**:Transmission function for three different lengths ($\varepsilon = -4$ eV, T=300K and $\beta = 0.74$ Å^{-1} [42]). **(b)**: V_m versus molecular length d. V_m becomes length independent for d>8 Å, consistent with the experiments by Beebe *et al.* [123, 124]. Inset:FN plots for the junctions in **a**.

5.4 Discussion

Before we discuss further consequences of this conclusion, we take a critical look at figure 5.3. Despite the qualitative agreement, the value of V_m predicted by the model is much higher than found in experiment (though much lower than the resonant value $V = 2\phi/e$). This can have several reasons. First, $E_F - E_{HOMO}$ may be considerably smaller than 4 eV. As discussed

above, there is quite some spread in the literature. Furthermore, the influence of image charges on molecular energy levels needs to be considered again. Just like in the Simmons case, the image force may yield a much lower level spacing for doubly contacted molecules as compared to free molecules. This phenomenon has recently attracted considerable theoretical attention [143, 144, 145, 146]. Finally, although our Lorentzian model does capture the basic physics behind molecular transport, detailed transport calculations will be needed to fully interpret TVS. Such studies should include the geometrical and electronic details of the molecular junction. For example, it was shown that the exact adsorption geometry of the molecule on the electrode has a pronounced effect on the shape of the transmission spectrum [147].

To finalize our discussion, let us return to figures 5.2 and 5.3. Clearly, the results for a coherent molecular model are radically different from those obtained for various Simmons models. There are two reasons for this. First, of course, the mathematics behind both models is not the same. Second, and perhaps more fundamental, the voltage profile is radically different. In the Simmons model, the potential decreases linearly with distance, whereas in the 'molecular' model, the voltage drops at the contacts only (see figure 5.1). It is easily visualized that the latter will result in a negligible length dependence of the shape of the $I(V)$-curves and thus in V_m being virtually independent of d. Interestingly, the very different properties of both models provide a fascinating perspective: TVS may allow us to distinguish molecular junctions from tunnel junctions without molecules. Perhaps surprisingly, such a tool is still generally lacking in (two-terminal) molecular transport. As shown above, the data by Beebe *et al.* can only be understood within a 'molecular' model. Inversely, this can also be seen as evidence for the fact that they did indeed probe a molecular system [148]. Clearly, a tunnel junction without molecules will obey Simmons characteristics, resulting in $V_m(d, \phi)$ relations like in figure 5.2. To test this proposition, we propose a series of experiments that consistently compares molecular junctions with tunnel junctions for various lengths and/or barrier energies.

5.5 Conclusion

We show that TVS is a very promising method for molecular transport. Nevertheless, the experimental data presented thus far, cannot be understood within vacuum tunneling (Simmons) models. Only within a coherent molecular transport model do we find qualitative consistency with experiment. Our results suggest that TVS is not only useful for spectroscopic means. In the future it may be employed to objectively check the presence of molecules in a junction.